

AD-A185 455

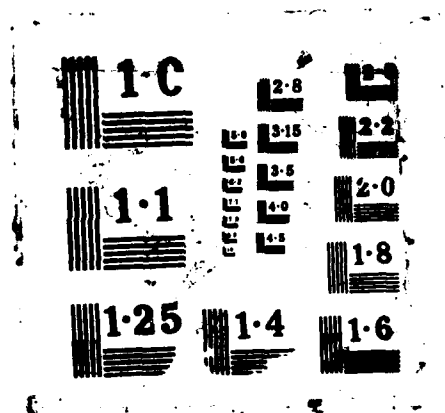
AN ABSOLUTE SCANNING (NF (ALPHA (1DELTA)) AND (NF  
(B(1EPSILON)) DIAGNOSTIC FOR THE N2F4 + H2 SYSTEM(U)  
AIR FORCE WEAPONS LAB KIRTLAND AFB NM Y D JONES JUN 87  
AFWL-TR-86-99 F/G 7/2

1/1

UNCLASSIFIED

NL

END  
007  
D/K



2

DTIC FILE COPY

AD-A185 455

AN ABSOLUTE SCANNING [NF ( $\alpha^1\Delta$ )] AND  
[NF ( $b^1\Sigma$ )] DIAGNOSTIC FOR THE  $N_2F_4 + H_2$   
SYSTEM

Y. D. Jones

June 1987

Final Report



Approved for public release; distribution unlimited.

AIR FORCE WEAPONS LABORATORY  
Air Force Systems Command  
Kirtland Air Force Base, NM 87117-6008

DTIC  
ELECTE  
OCT 5 1987  
S B D

87 9 29

038

UNCLASSIFIED

SECURITY CLASSIFICATION OF THIS PAGE

AD-A185455

## REPORT DOCUMENTATION PAGE

1a. REPORT SECURITY CLASSIFICATION			1b. RESTRICTIVE MARKINGS		
2a. SECURITY CLASSIFICATION AUTHORITY			3. DISTRIBUTION / AVAILABILITY OF REPORT Approved for public release; distribution unlimited.		
2b. DECLASSIFICATION / DOWNGRADING SCHEDULE					
4. PERFORMING ORGANIZATION REPORT NUMBER(S)  AFWL-TR-86-99			5. MONITORING ORGANIZATION REPORT NUMBER(S)		
6a. NAME OF PERFORMING ORGANIZATION  Air Force Weapons Laboratory		6b. OFFICE SYMBOL (If applicable)		7a. NAME OF MONITORING ORGANIZATION	
6c. ADDRESS (City, State, and ZIP Code)  Kirtland Air Force Base, New Mexico 87117-6008			7b. ADDRESS (City, State, and ZIP Code)		
8a. NAME OF FUNDING / SPONSORING ORGANIZATION		8b. OFFICE SYMBOL (If applicable)		9. PROCUREMENT INSTRUMENT IDENTIFICATION NUMBER	
8c. ADDRESS (City, State, and ZIP Code)			10. SOURCE OF FUNDING NUMBERS		
			PROGRAM ELEMENT NO. 62601F	PROJECT NO. 3326	TASK NO. 03
			WORK UNIT ACCESSION NO. 85		
11. TITLE (Include Security Classification)  AN ABSOLUTE SCANNING [NF(a <sup>1</sup> Δ)] AND [NF(b <sup>1</sup> Σ)] DIAGNOSTIC FOR THE N <sub>2</sub> F <sub>4</sub> + H <sub>2</sub> SYSTEM					
12. PERSONAL AUTHOR(S) Y. D. Jones					
13a. TYPE OF REPORT Final		13b. TIME COVERED FROM 1/1/85 TO 1/1/86		14. DATE OF REPORT (Year, Month, Day) 1987, June	
15. PAGE COUNT 20					
16. SUPPLEMENTARY NOTATION					
17. COSATI CODES			18. SUBJECT TERMS (Continue on reverse if necessary and identify by block number)		
FIELD	GROUP	SUB-GROUP	Nitrogen Fluoride Diagnostics		
07	04		Excited State Infrared Emission		
			Spectroscopy		
19. ABSTRACT (Continue on reverse if necessary and identify by block number)  The N <sub>2</sub> F <sub>4</sub> + H <sub>2</sub> system is of interest for production of NF(a <sup>1</sup> Δ) as an energy transfer species. Past studies have been plagued with the difficult NF(a <sup>1</sup> Δ) quantitative measurement due to interferences from the close-lying N <sub>2</sub> (B) and HF peaks. This paper deals with the development of a scanning diagnostic to determine concentrations of NF(a <sup>1</sup> Δ) and NF(b <sup>1</sup> Σ) in the N <sub>2</sub> F <sub>4</sub> + H <sub>2</sub> system and quantitative measurement of interferences with the diagnostic signal. The diagnostic was then applied to a functioning high-pressure, high-temperature system.					
20. DISTRIBUTION / AVAILABILITY OF ABSTRACT <input checked="" type="checkbox"/> UNCLASSIFIED/UNLIMITED <input type="checkbox"/> SAME AS RPT. <input type="checkbox"/> DTIC USERS			21. ABSTRACT SECURITY CLASSIFICATION Unclassified		
22a. NAME OF RESPONSIBLE INDIVIDUAL Capt. Glen Perram			22b. TELEPHONE (Include Area Code) (505) 844-1871		22c. OFFICE SYMBOL ARDA

DD FORM 1473, 84 MAR

83 APR edition may be used until exhausted.  
All other editions are obsolete

SECURITY CLASSIFICATION OF THIS PAGE

UNCLASSIFIED

UNCLASSIFIED

SECURITY CLASSIFICATION OF THIS PAGE

UNCLASSIFIED

SECURITY CLASSIFICATION OF THIS PAGE



## ILLUSTRATIONS

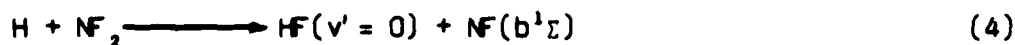
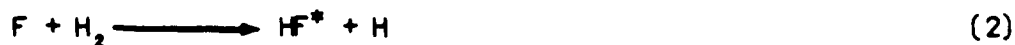
<u>Figure</u>		<u>Page</u>
1	Schematic of the NF( $a^1\Delta$ ) and NF( $b^1\Sigma$ ) diagnostics	4
2	Experimental setup of the diagnostics	6
3	Digitized photograph of the actual device flame	8
4	OMA III scan of the HF emission	8
5	OMA III scan of the NF( $a^1\Delta$ ) and HF region with an overlay of the band-pass filter transmission curve	9
6	Monochromator scan of the NF( $a^1\Delta$ ) region with an overlay of the band-pass filter transmission	10
7	Sample NF( $a^1\Delta$ ) scan with the diagnostic	12
8	Sample NF( $b^1\Sigma$ ) scan with the diagnostic	12

## I. INTRODUCTION

The  $N_2F_4 + H_2$  chemical production scheme for  $NF(a^1\Delta)$  and  $N_2(A)$  is of interest because of the large amount of energy stored in both molecules. The  $NF(a^1\Delta)$  concentration in these systems has been difficult to determine due to the close-lying peaks of the  $N_2(B)$  and HF spectra. This report describes reliable  $NF(a^1\Delta)$  and  $NF(b^1\Sigma)$  diagnostics. The  $N_2(B)$  and HF interferences in our system have been identified and quantified. These studies have provided an accurate method of determining  $NF(a^1\Delta)$  in high densities, as well as  $NF(b^1\Sigma)$  in moderate concentrations.

The  $NF(a^1\Delta)$  molecule is long-lived at 5.6 seconds (Ref. 1) and has an internal energy of  $11500\text{ cm}^{-1}$  available for transfer.  $NF(b^1\Sigma)$ , also produced in this system, has a lifetime of 23 ms (Ref. 2). The  $NF(a)$  and  $NF(b)$  states were detected using spontaneous emission detection by absolute radiometry. The  $NF(a^1\Delta) \rightarrow NF(X^3\Sigma)$  at 874.2-nm transition and the  $NF(b^1\Sigma) \rightarrow NF(X^3\Sigma)$  at 528.8-nm transition were used to monitor the concentrations in a supersonic flow regime.

The reactions in the  $N_2F_4 + H_2$  system leading to  $NF(a^1\Delta)$  and  $NF(b^1\Sigma)$  are summarized in Eqs. 1 through 5.



1. Malins, R. J., and D. W. Senser, J. Chem. Phys. **85**, 1342 (1981).
2. Cheah, C. T., and M. A. A. Clyne, J. Photochem. **15**, 21 (1981) and P. H. Tennyson, A. Fontijn, and M. A. A. Clyne, J. Chem. Phys. **62**, 171 (1981).



The diagnostic was incorporated in the study of the overall  $\text{N}_2\text{F}_4 + \text{H}_2$  production scheme for  $\text{N}_2^+$ . The operating regime for the diagnostic was detection of high densities in supersonic, high-temperature flows. The device and additional diagnostics will be described in a future report.

## II. DESIGN

The diagnostic incorporated a 0.953-cm-diam tube, 38.1 cm long. Both ends were fitted with 0.17-cm-diam orifices held in place by tubing fittings. A bifurcated fused silica fiber optic cable (Oriel) was fixed in the fitting on one end of the tube. The tube or spatial filter was then attached to a translation stage. The position of the translation stage, and thus the spatial filter, was determined from the output from a calibrated linear voltage displacement transducer (LVDT).

The setup for the diagnostics is shown in Figure 1. The  $NF(a^1\Delta)$  emission was detected by a thermoelectrically cooled RCA C31034A photomultiplier tube (PMT) which was attached to one of the bifurcated cable ends. Between the fiber optic and the PMT was a very narrow band-pass filter (Barr Associates) centered at 874.29 nm with a full width at half maximum (FWHM) of 0.98 nm. Maximum transmission was 0.52. The  $NF(b^1\Sigma)$  was detected by emission passing through the other side of the cable, a band-pass filter (Corion) centered at 531.4 nm with a FWHM of 9.8 nm and maximum transmission of 0.54, and to a thermoelectrically cooled RCA 4837 PMT. Each PMT was optimized for response with regard to both voltage applied and temperature of the cooled housing.

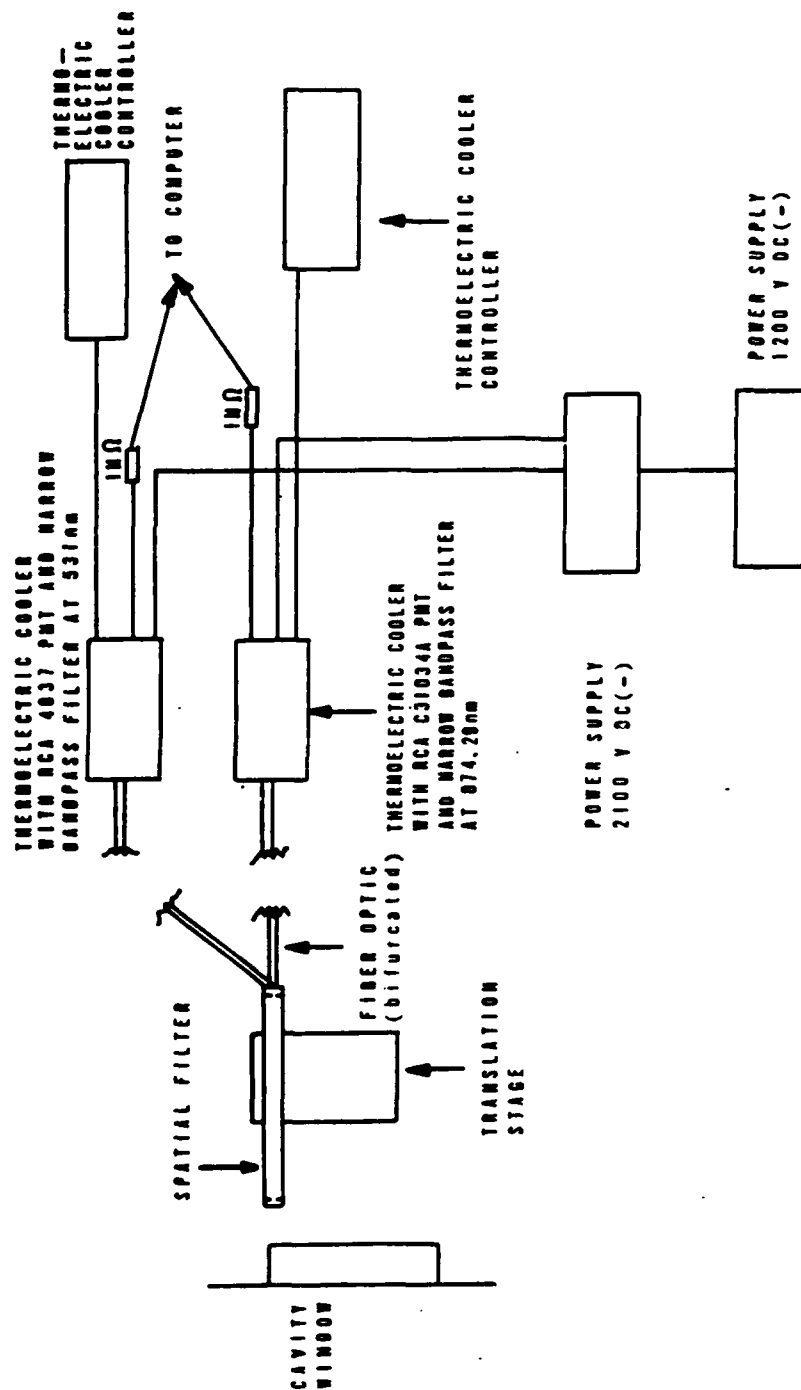


Figure 1. Schematic of the NF( $a^1\Delta$ ) and the NF( $b^1\Sigma$ ) diagnostics.

## III. CALIBRATION

## STANDARD LAMP CALIBRATION

Calibration of the diagnostics was performed using a quartz-halogen-tungsten FEL-type lamp, the calibration of which was performed with an NBS standard (Eppley Laboratory, Inc.). The lamp was periodically checked in-house against an NBS secondary standard. The lamp was run at 7.9 A.

The calibration procedure and geometry considerations have been previously described (Ref. 3). To summarize, the differential radiated power,  $dP$ , which reaches the rear aperture of the spatial filter is given by

$$dP = [NF^*] h\nu k_T \frac{f(r, z) A \cos\theta}{4\pi(r^2 + z^2)} dV \quad (6)$$

where

$[NF^*]$  = molecules/cm<sup>3</sup> of either NF(a<sup>1</sup>Δ) or NF(b<sup>1</sup>Σ)

$h\nu$  = Energy of a photon at the emission frequency

$k_T$  = Radiative rate of the transition

$A$  = Rear aperture area (cm<sup>2</sup>)

$\frac{f(r, z) A \cos\theta}{4\pi(r^2 + z^2)}$  = Solid angle subtended at the rear aperture by the differential volume element with radius =  $(r^2 + z^2)^{1/2}$

$\theta$  = angle between the z-axis and the radius vector that connects the origin to the differential volume element

$f(r, z)$  = occlusion factor

Figure 2 shows the experimental arrangement of the diagnostic. The shape of the flame was monitored via a video camera and digitized to determine the

3. Johnson, D., R. Meyer, Y. D. Jones and G. Hager, Laser Digest, to be published.

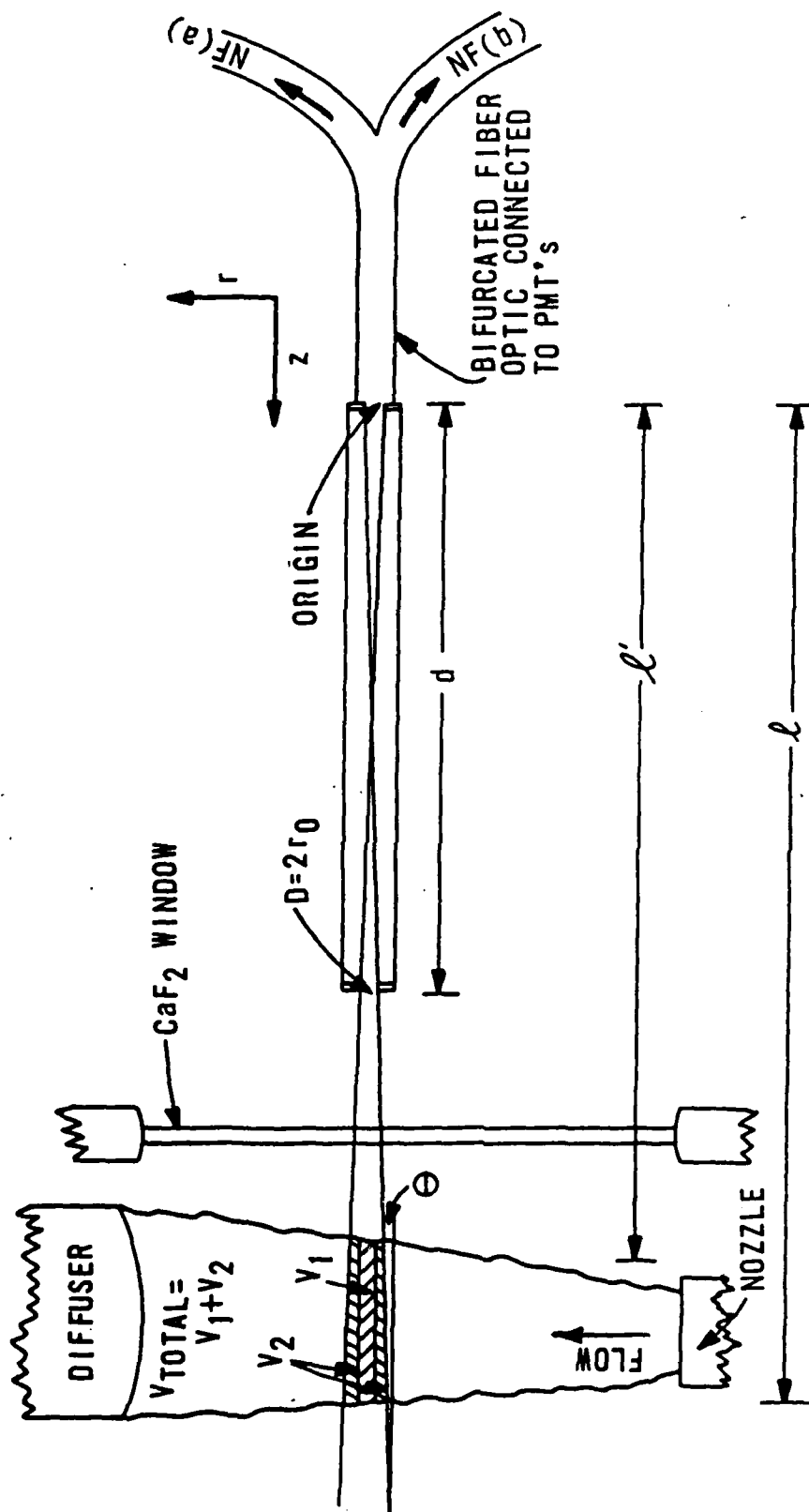


Figure 2. Experimental setup of the diagnostics.

precise collection volume along the scan (Fig. 3). Through several manipulations as given in Reference 3, the number of photons/s landing on the detector,  $N^*$ , is given by

$$N^* = \frac{P'}{h\nu} = \frac{T[NF^*]h\nu k_T A}{4\pi} \cdot \left[ 2\pi \int_L^L \int_0^{r_0} \frac{zr \, dzdr}{(r^2 + z^2)^{3/2}} + \pi \int_L^L \int_{r_0}^{2rz/d - r_0} \frac{zr \, dzdr}{(r^2 + z^2)^{3/2}} \right] \quad (7)$$

where  $T$  is the total transmission of any filters used in the diagnostic plus the transmission of the cavity window.

#### VERIFICATION OF POSSIBLE INTERFERENCES FROM CLOSE-LYING PEAKS IN THE $NF(a^1\Delta)$ DIAGNOSTIC

To determine the amount of interference from the  $HF(3-0)$  emission, a moderate resolution spectra was obtained using an OMA III (EG&G PAR) with a 1200  $\lambda/\text{mm}$  grating. Figure 4 shows a scan with just the combustor, used to produce F atoms, operating. It was assumed that the majority of  $HF^*$  originated from the combustor. Only the region of interest from 870 nm to 900 nm is shown. Figure 5 shows a scan with  $NF(a^1\Delta)$  and  $N_2(B)$  being produced. The  $HF$  distribution appears to change very little in intensity when  $N_2F_4 + H_2$  is added. This comparison was made over a wide variety of  $N_2F_4$  and secondary  $H_2$  flows. The results were consistent within our flow conditions; therefore, a simple subtraction of the  $HF$  contribution yielded a reliable correction factor for  $HF$ .

Scans to determine the population in the  $N_2(B, v' - v'') = 1 - 0, 0 - 0$  and  $0 - 1$  were performed using a 0.3-m monochromator (Acton) with a 1200  $\lambda/\text{mm}$  grating blazed at 1.0  $\mu\text{m}$ . The monochromator was equipped with an intrinsic germanium detector (Applied Detector Corporation). The scans showed little or no interference, with our flow conditions, from the  $N_2(B, 1 - 0)$  peak. The scans showed the population in the strong  $0 - 0$  peak to be very low

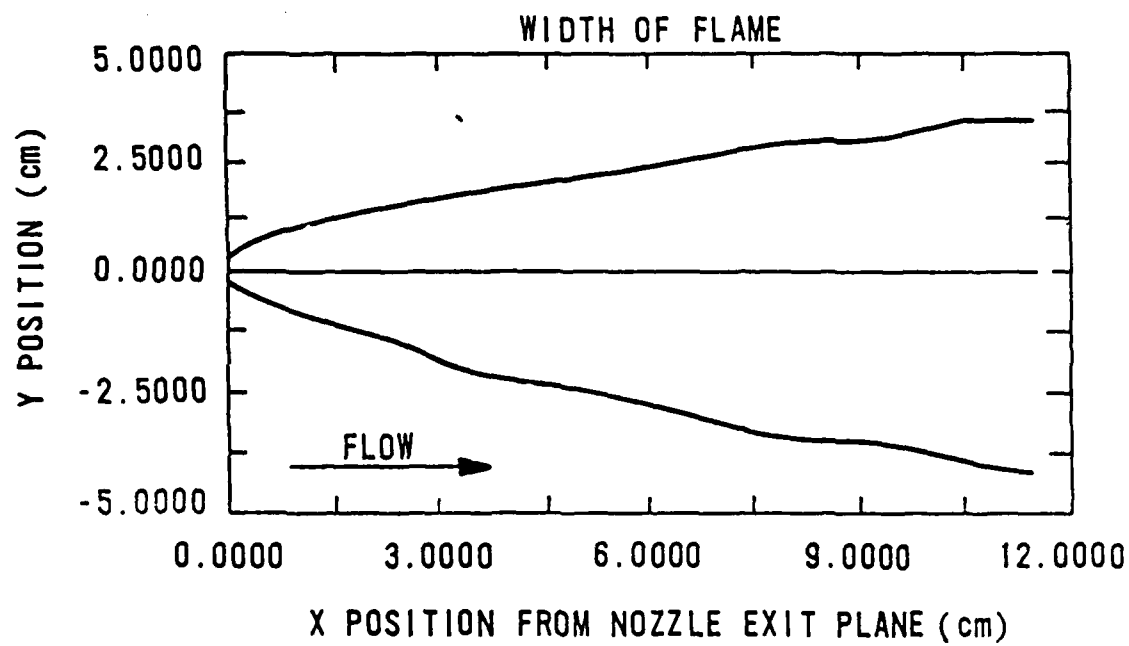


Figure 3. Digitized photograph of the actual device flame.

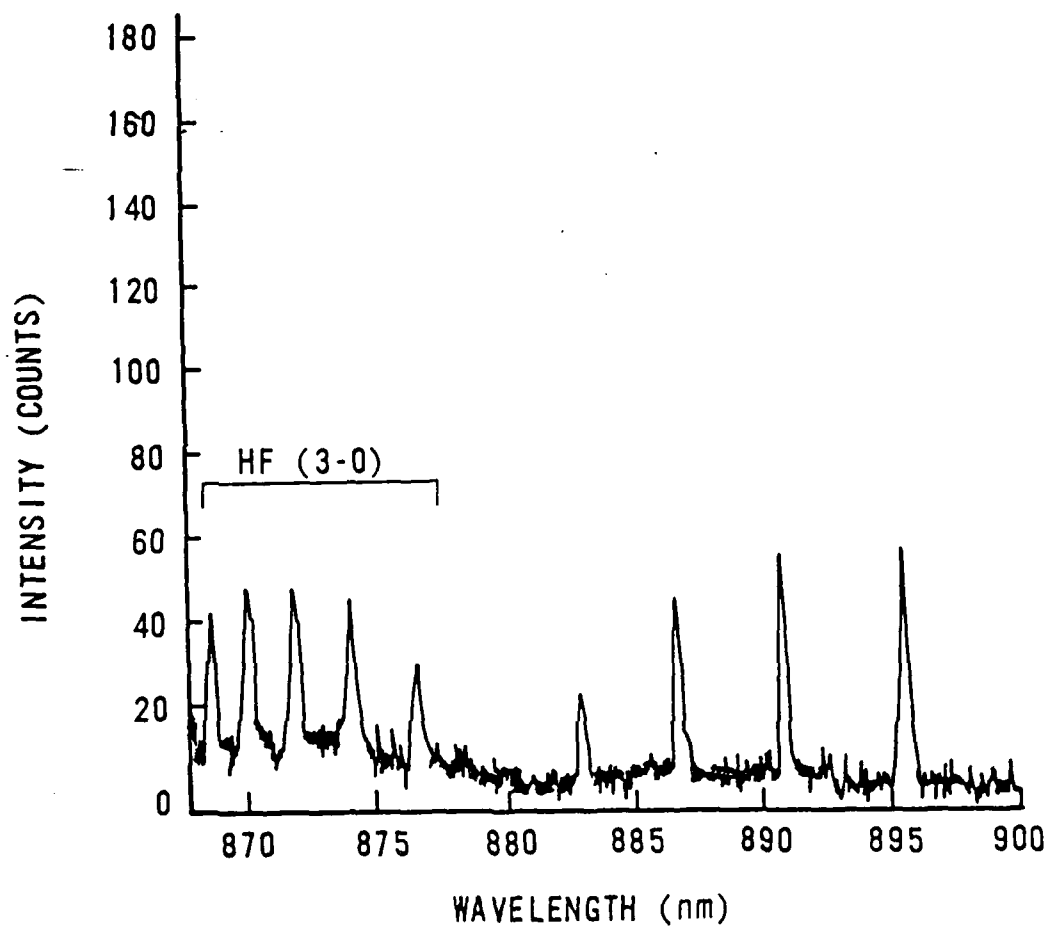


Figure 4. OMA III scan of the HF emission.

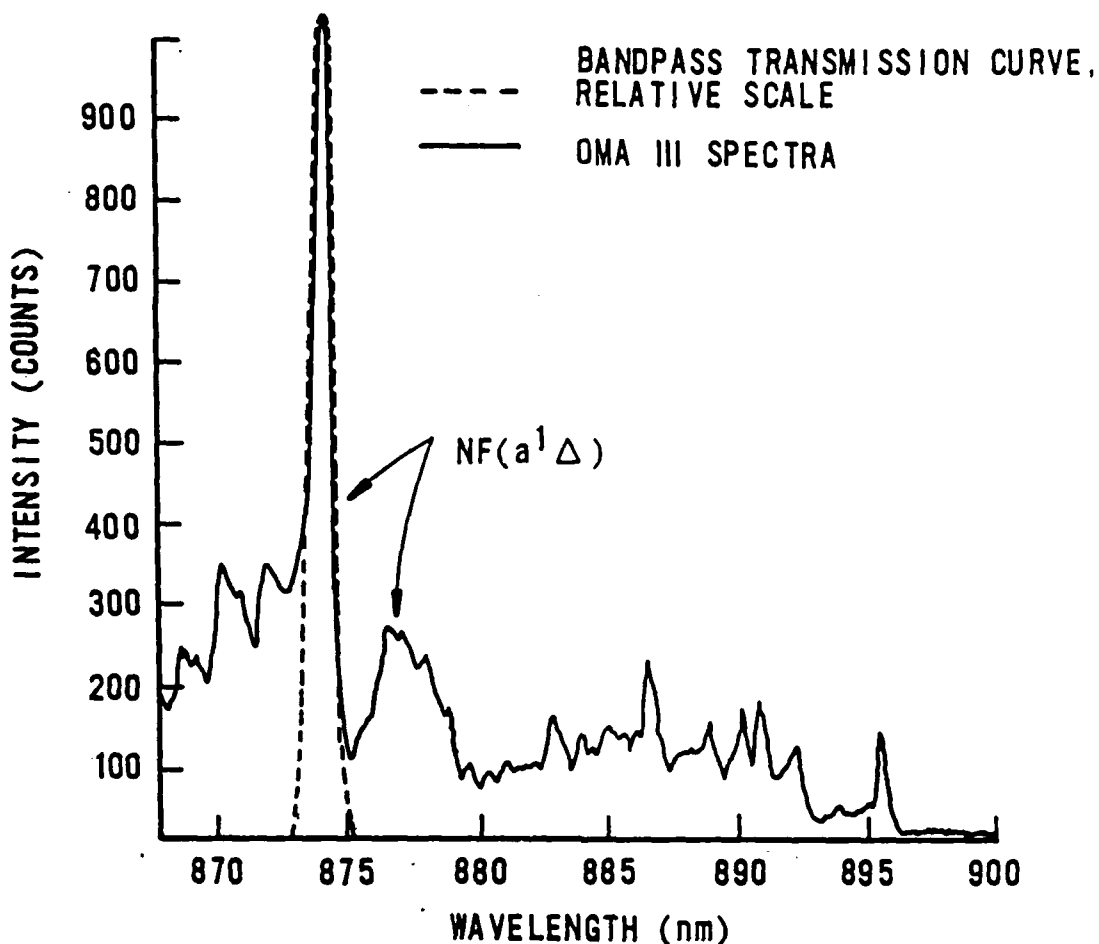


Figure 5. OMA III scan of the NF ( $a^1\Delta$ ) and HF region with an overlay of the band-pass filter transmission curve.

(approximately  $10^8$  molecules/cm<sup>3</sup>), which substantiated the minimal interference from the 1 - 0 peak.

The monochromator scans allowed for a more accurate separation of the HF and NF(a) peaks as well. The result was that the HF contribution to the NF(a) diagnostic signal never exceeded 33 percent of the diagnostic signal; however, the average contribution was around 10 percent for our flow conditions. The  $N_2(B)$  and HF population were monitored for each type of run condition. Therefore, the exact contribution to the NF( $a^1\Delta$ ) diagnostic could be subtracted out. A monochromator scan with the trace of the narrow band-pass filter transmission curve is shown in Figure 6. The area under the spectral curve was multiplied by the band-pass transmission to obtain actual interferences in specific flow conditions.



--- BANDPASS FILTER TRANSMISSION CURVE

— WORST FLOW CASE  
SCAN WITH 0.3m MONOCHROMATOR  
500 nm BLAZED, 1200  $\lambda$ /mm GRATING  
50 $\mu$  SLITS

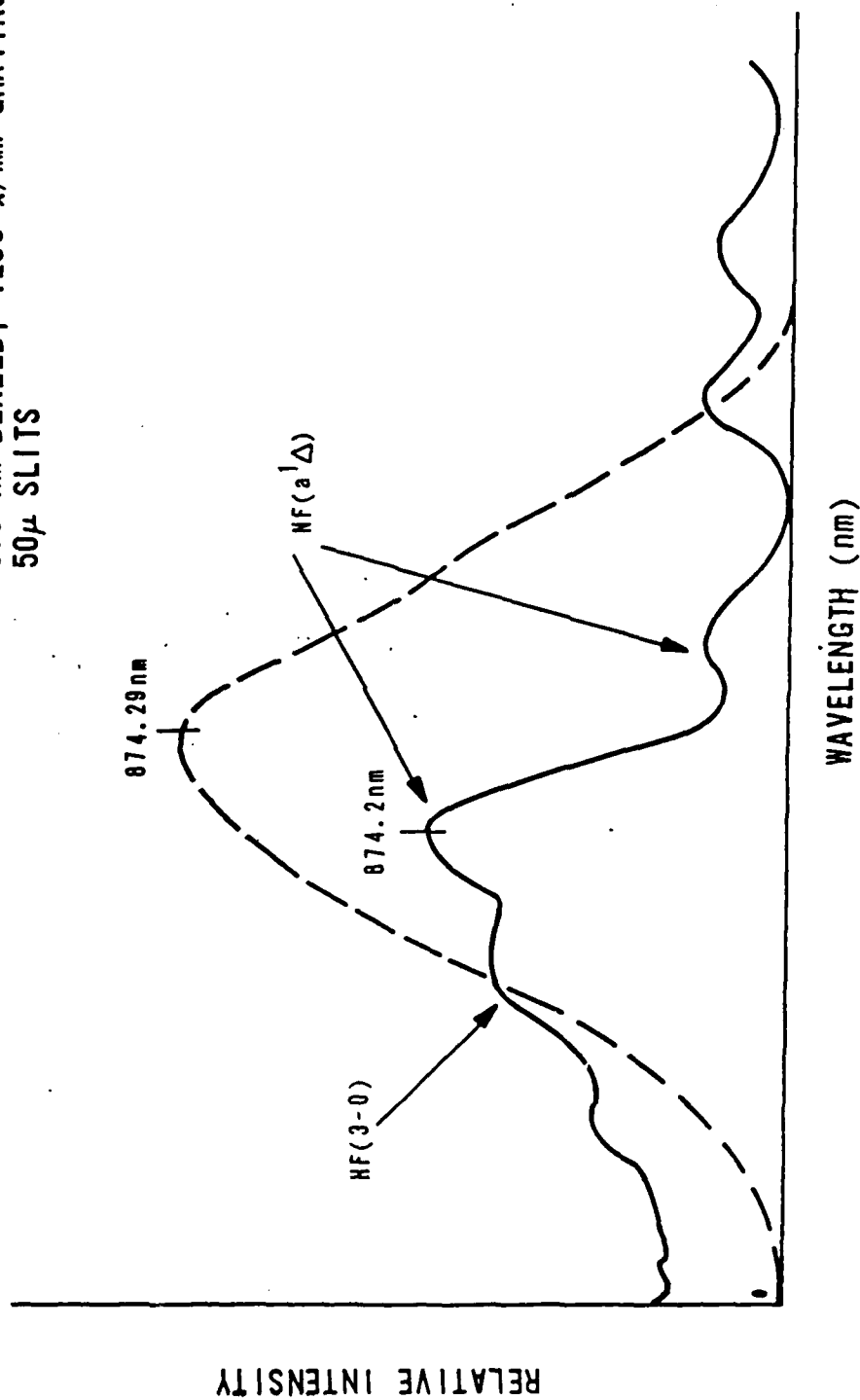


Figure 6. Monochromator scan of the NF( $a'\Delta$ ) region with an overlay of the band-pass filter transmission.

## IV. RESULTS

The  $\text{NF}(a^1\Delta)$  and  $\text{NF}(b^1\Sigma)$  diagnostics were extremely useful in determining the yield of the  $\text{N}_2\text{F}_4 + \text{H}_2$  chemical production system. Figures 7 and 8 contain sample scans of the diagnostics along the centerline of the flow field. The detection capability of the  $\text{NF}(a^1\Delta)$  was from  $10^{14}$  to  $10^{16}$  molecules/cm<sup>3</sup> in the current arrangement, with an error of  $\pm 20$  percent. Error in determining the active volume actually sampled by the diagnostic is close to 10 percent. The errors in determining the exact ratio of interferences to the  $\text{NF}(a^1\Delta)$  signal are within 10 percent. At this time there is some question as to whether the  $\text{NF}(a^1\Delta)$  lifetime is correct; however, until the lifetime is verified, that error cannot be assessed. Once the lifetime is determined, the diagnostic calibration may simply be corrected. The  $\text{NF}(b^1\Sigma)$  diagnostic had a range from  $10^{11}$  to  $10^{13}$  molecules/cm<sup>3</sup> and an error of  $\pm 10$  percent, arising mostly from determining the geometry of the sampled volume.

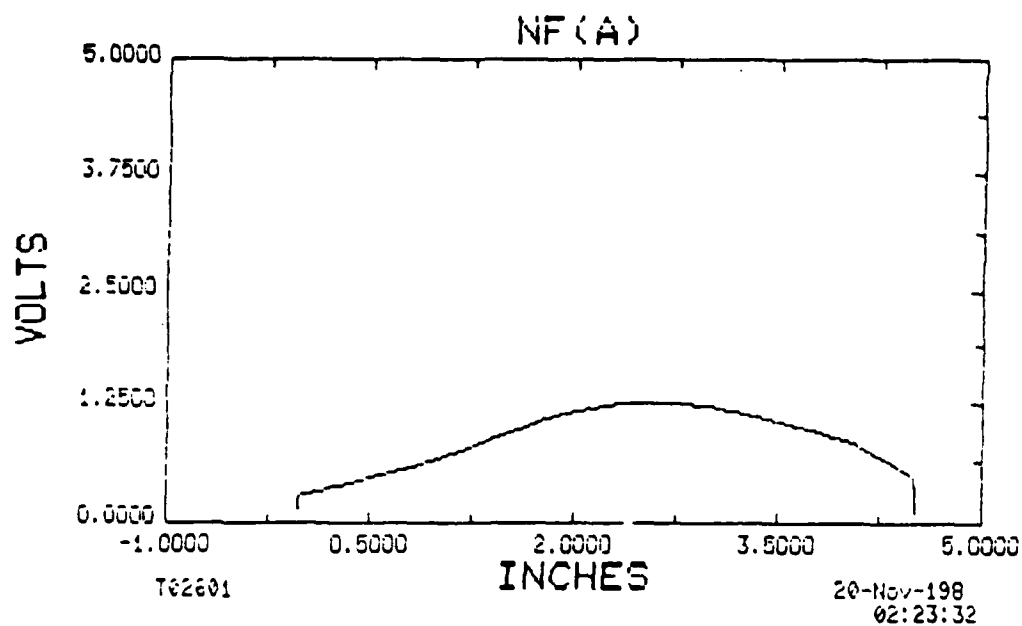


Figure 7. Sample NF( $a^1\Delta$ ) scan with the diagnostic.

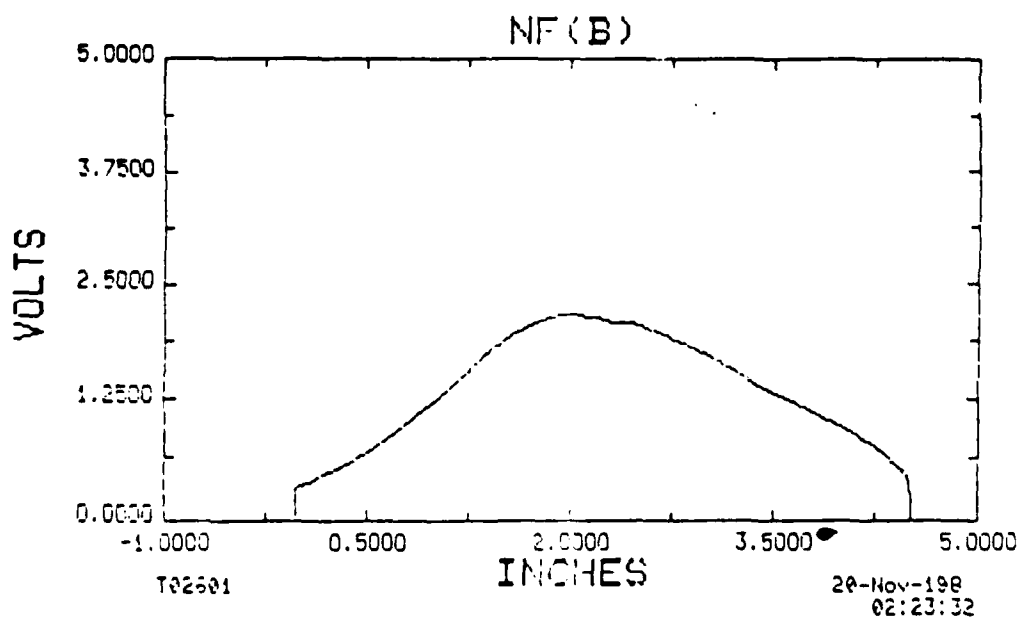


Figure 8. Sample NF( $b^1\Sigma$ ) scan with the diagnostic.

## V. CONCLUSIONS AND RECOMMENDATIONS

The  $\text{NF}(a^1\Delta)$  and  $\text{NF}(b^1\Sigma)$  diagnostics have been critical in determining the overall production of the two species as well as the species distribution across the flow field. The  $\text{NF}(a^1\Delta)$  diagnostic requires in-depth analysis of the medium before application. It is especially important to determine all possible interferences from other species emission. The application of this diagnostic to the  $\text{N}_2\text{F}_4 + \text{H}_2$  system led to a reexamination of the branching ratio as defined by Eqs. 3 and 4. The branching ratio is currently being investigated.

END

11-87

DTIC